



ELECTRONIC PROPERTIES OF Ca AND Mg CoDoped ANATASE TiO₂: A DFT STUDY

Mbae Jane Kathure¹, Njagi Eric¹, Muthui Zipporah Wanjiku^{1a)}

¹Chuka University, P.O. Box 109, 60400 Chuka, Kenya

^{a)} Corresponding Author

Article DOI: <https://doi.org/10.36713/epra23842>

DOI No: 10.36713/epra23842

ABSTRACT

In the constant pursuit for green energy sources, there is a growing focus on materials that utilize solar energy efficiently in processes such as photocatalysis. TiO₂ is one of the most widely studied semiconductor material that is suitable for photocatalytic applications. In particular, the anatase phase of TiO₂ has been reported to demonstrate superior photocatalytic performance compared to other naturally existing polymorphs, rutile and brookite. With a wide energy band gap however, of ≈ 3.2 eV, it is limited to be active in the UV region of the electromagnetic spectrum, which constitutes $\approx 4\%$ of the solar energy spectrum. To improve its solar energy utilization efficiency, the effect of codoping alkaline earth metal acceptor dopant cations Mg²⁺ and Ca²⁺ within the TiO₂ anatase lattice on the electronic properties has been investigated using the Density Functional Theory (DFT) method, using the state of the art Quantum ESPRESSO code. Dopant impurity states are introduced at the edge of the valence states which are lifted to higher energies and intersect the Fermi level upon alkaline earth metal codoping, an electronic structure modification that has been reported to improve the visible light responsiveness of the photocatalyst.

KEYWORDS: Anatase, DFT, Quantum ESPRESSO, Electronic properties

1.0 INTRODUCTION

Titanium (IV) Oxide (TiO₂) exhibits properties that have potential technological applications such as in photocatalysis [1] [2], [3], [4]. Being a polymorphic material, it exists in various phases such as the fluorite, pyrite, rutile, anatase, hollandite, brookite, ramsdellite, columbite, cotunnite, modified fluorite, bronze, baddeleyite and hexagonal Fe₂P-type phases [5]. The anatase phase has been reported to be a more active photocatalyst [6]. Among the factors associated with the higher photocatalytic activity is the increased oxidation strength of the photoexcited electrons, owing to the larger band gap of anatase. The indirect band gap in the band structure of anatase is also reported to increase the lifetime of the charge carriers. In addition, the average effective mass for electrons and holes in anatase has been reported to be smaller, subsequently facilitating their migration, thereby reducing the charge recombination rate [2].

As a photocatalyst, TiO₂ has been used for environmental applications for treatment of water and to obtain ultraclean water suitable for the pharmaceutical industry and microelectronics. It mineralizes organic substances in aqueous and air phase, completely, often to carbon dioxide, water, nitrates, chalcogenides, phosphates, and other inorganic ions, depending on the nature of the pollutant [7], [8].

To improve the photocatalytic performance of TiO₂, techniques such as introduction of impurity defects through mono and codoping strategies have been explored by various researchers. Both cations and anions have been reported to enhance the photocatalytic properties of TiO₂, with codoping techniques being shown to be more promising. The observed electronic structure modifications responsible for the improved photocatalytic response have been generation of impurity states below the conduction band minimum of the energy band gap [9].

Metal-metal, nonmetal-nonmetal, and metal-nonmetal ion combinations have been reported in literature, with transition metal-nonmetal codoping in TiO₂ being reported to reduce charge recombination, thereby increasing photocatalytic activity in the visible light region [10]. Nonmetal-nonmetal, metal-nonmetal and metal-metal codopant pairs such as N-P, Cr-N and Sn-Nb, respectively, have been reported to reduce the band gap of TiO₂ to 1.8 eV, 1.5 eV and 3.04 eV respectively from 3.2 eV, an effect that is favorable for visible light response. Introduction of donor-acceptor codopants such as Nb⁵⁺- Rh³⁺, which are ions with more and less valence electrons respectively, compared to Ti⁴⁺, in TiO₂ has been explored and demonstrated to reduce charge effects that are commonly observed with monodoping through charge compensation [9].

Ongoing research efforts continue to be made to reveal new possibilities and the enhancement of the electronic structure modification of TiO₂ remains to be an active research topic, as the need for improved properties persists. In this study, the effect of introducing nontoxic dopants, alkaline earth metal cations, Mg and Ca has been investigated. Electronic structure modifications have been revealed



in the Total Density of States (TDOS) plots, which has been reported in literature to improve the visible light response of photocatalysts [6].

2.0 COMPUTATIONAL DETAILS

A $2 \times 2 \times 2$ anatase TiO_2 supercell having 96 atoms, with a tetragonal structure, space group I41/amd was modelled using the Visualization for Electronic Structural Analysis (VESTA) visualization software. The optimized lattice parameters of $a = b = 3.816 \text{ \AA}$ and $c = 9.693 \text{ \AA}$ were used to perform the electronic structure calculations. Doping was carried out by substituting Ti with the divalent Mg and Ca alkaline earth metal codopants within the TiO_2 anatase lattice. Density functional theory (DFT) calculations were carried out using plane wave basis sets and pseudopotentials as implemented in the Quantum ESPRESSO open source simulation package. The optimized plane waves cutoff energy of 40 Ry was used, while the core-valence interaction was treated using ultrasoft pseudopotentials (USPPs). The exchange-correlation was treated using the generalised gradient approximation (GGA), employing the Perdew–Burke–Ernzerhof (PBE) exchange-correlation functional (PBE-GGA). K-Point sampling used a $(3 \times 3 \times 2)$ Monkhorst–Pack sampling grid to carry out the integration using the linear tetrahedron method with Bloechl’s corrections over the irreducible Brillouin zone and the Marzari–Vanderbilt smearing scheme with a Gaussian spreading of 0.05 Ry. The evaluation of the solution to the Kohn–Sham equation iterations ended at a convergence criterion of 10^{-8} eV . The maximum number of geometric and electronic iterations was set at 100. Generally, all calculations began from scratch.

3.0 RESULTS

The energy band gap of pristine anatase is shown in Fig. 1. The indirect band gap is evident, and no states intersect the Fermi level.

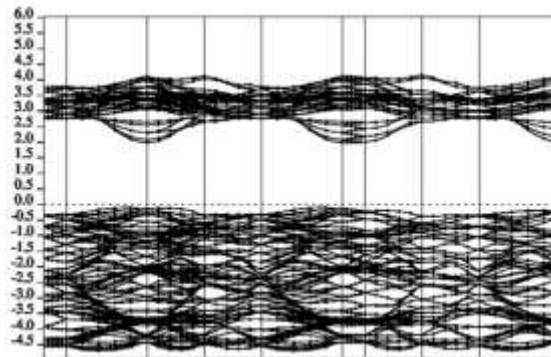


Fig. 1: Anatase Band Structure

Upon single cationic simultaneous substitution with divalent alkaline earth metal dopant cations, Mg and Ca, in place of Ti, which corresponds to a 3.125% Mg + 3.125% Ca dopant concentration, the edge of the valence states is observed to intersect the Fermi level slightly as shown in Fig. 2.

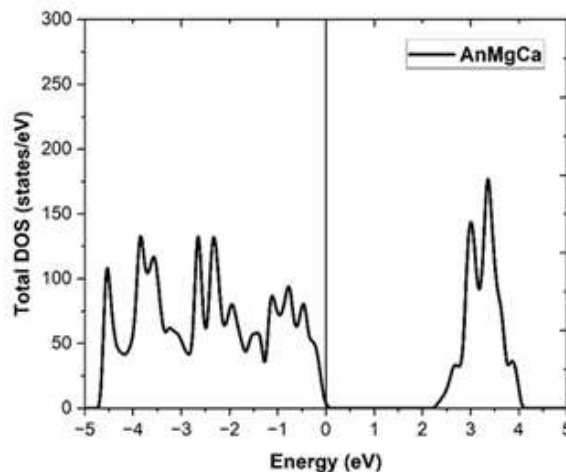


Fig. 2: Total Density of States (TDOS) of 3.125% Mg + 3.125% Ca doped anatase TiO_2

The intersection of the Fermi level is much more noticeable for a higher dopant concentration of 6.25%Mg + 6.25% Ca as shown in Fig. 3

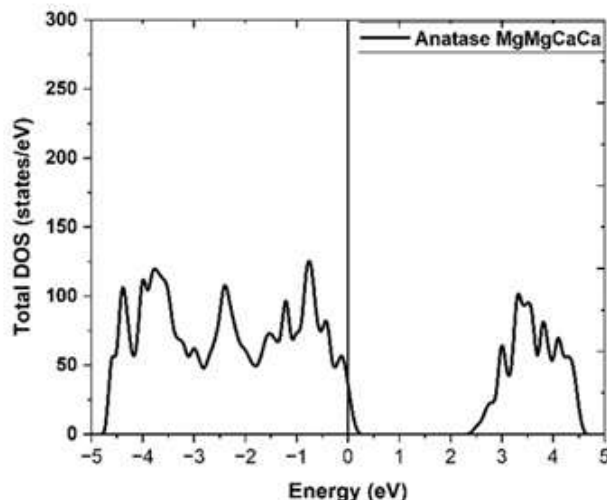


Fig. 3: Total Density of States (TDOS) of 6.25%Mg + 6.25% Ca doped anatase TiO₂

A magnesium rich doped system shifted the valence edge to higher energies to a greater extent as compared to a Ca rich doped system as shown in Fig. 4.

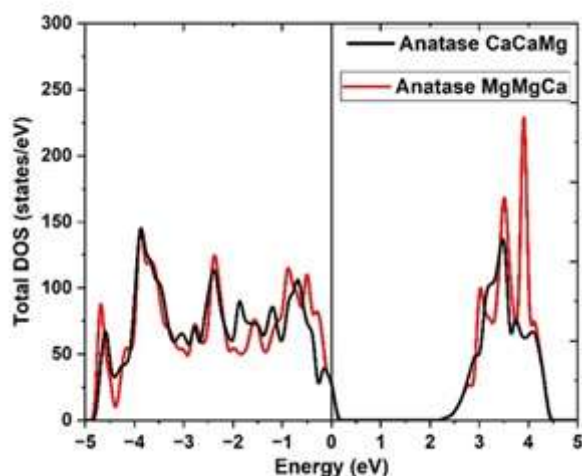


Fig. 4: Total Density of States (TDOS) of 6.25%Mg + 3.125% Ca doped anatase TiO₂(Red line) & 3.125%Mg + 6.25% Ca doped anatase TiO₂(black line)

Codoping Mg and Ca within the anatase TiO₂ lattice causes a significant modification of the electronic structure. The changes are observed at the Fermi level, with the valence states shifting to higher energies, hence intersecting the Fermi level. This effect increases with dopant concentration and is expected to result in an improved visible light response of the doped photocatalysts. Both Mg and Ca have a larger ionic radii as compared to Ti at 72 pm, 100 pm [11] and 60.5pm for Mg²⁺, Ca²⁺ and Ti⁴⁺ respectively [4]. Bigger ions such as Y³⁺ have been reported to expand the lattice parameters and induce a red shift of the Raman peak [9].

Fig. 5 shows a close up picture of the nature of the orbital contribution of the wavefunctions at the Fermi level in the Projected Density of States (PDOS) for all the atoms in the doped system.

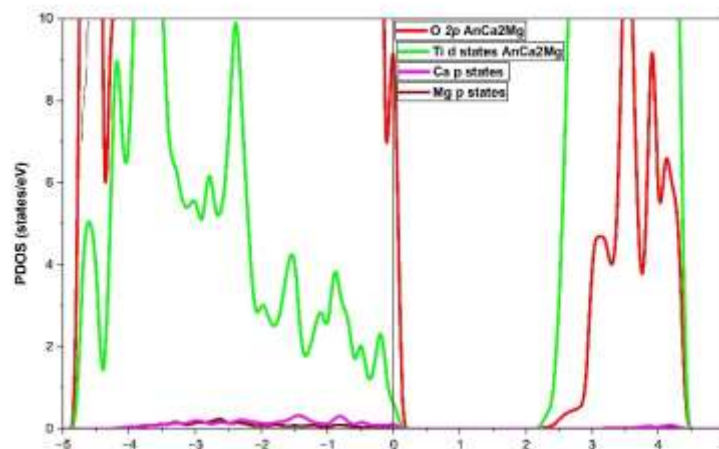


Fig. 5: Projected Density of States (PDOS) for Ti, O, Mg and Ca in 6.25%Mg + 3.125% Ca doped anatase TiO₂

Unoccupied O $2p$ states are evident just above the Fermi level. This observation is expected, owing to the effect of divalent dopants substituting Ti^{4+} cations. The electron deficit results in the generation of two holes per dopant ion, resulting in oxygen unoccupied states [12], [13]. The overlap of the Mg and Ca dopant states with the parent Ti and O states within the same energy region leads to hybridization of the states within the doped system [14], and results in a lifting of the valence edge states to higher energies. This observation at the atomic scale explains experimental observations, in which acceptor dopants cause the formation of oxygen vacancies, which have as well been associated with improved visible light harvest in the structurally defective systems.

CONCLUSION

Codoping of anatase TiO₂ with alkaline earth metal divalent ions Mg²⁺ and Ca²⁺ results in a lifting of the edge of the valence states to higher energies with negligible effect on the edge of the unoccupied states. The dopant states overlap with the parent states causing a charge distribution occasioned by the electron deficit arising from substituting 4+ ions with divalent cations in the anatase TiO₂ lattice. These electronic structure modifications have been associated with improved visible light harvest, charge carrier separation, diffusion, transport, catalytic efficiency and mass transfer phenomena.

REFERENCES

1. M. Elahifard, M. R. Sadrian, A. Mirzanejad, R. Behjatmanesh-Ardakani, and S. Ahmadvand, "Dispersion of Defects in TiO₂ Semiconductor: Oxygen Vacancies in the Bulk and Surface of Rutile and Anatase," *Catalysts*, vol. 10, no. 4, 2020, doi: 10.3390/catal10040397.
2. Ž. Kovačič, B. Likozar, and M. Huš, "Electronic properties of rutile and anatase TiO₂ and their effect on CO₂ adsorption: A comparison of first principle approaches," *Fuel*, vol. 328, p. 125322, Nov. 2022, doi: 10.1016/j.fuel.2022.125322.
3. N. S. Portillo-Vélez, O. Olvera-Neria, I. Hernández-Pérez, and A. Rubio-Ponce, "Localized electronic states induced by oxygen vacancies on anatase TiO₂ (101) surface," *Surf. Sci.*, vol. 616, pp. 115–119, 2013, doi: <https://doi.org/10.1016/j.susc.2013.06.006>.
4. N. Thongyong, P. Thongbai, and P. Srepusharawoot, "DFT calculations and giant dielectric responses in (Ni_{1/3}Nb_{2/3})_xTi_{1-x}O₂," *RSC Adv*, vol. 13, no. 45, pp. 31844–31854, 2023, doi: 10.1039/D3RA06541C.
5. Q.-J. Liu, Z. Ran, F.-S. Liu, and Z.-T. Liu, "Phase transitions and mechanical stability of TiO₂ polymorphs under high pressure," *J. Alloys Compd.*, vol. 631, pp. 192–201, 2015, doi: <https://doi.org/10.1016/j.jallcom.2015.01.085>.
6. K. Mbae and Z. W. Muthui, "Ab initio Investigation of the Structural and Electronic Properties of Alkaline Earth Metal - TiO₂ Natural Polymorphs," *Adv. Mater. Sci. Eng.*, vol. 2022, no. 1, p. 7629651, 2022, doi: <https://doi.org/10.1155/2022/7629651>.
7. S. J. Armaković, M. M. Savanović, and S. Armaković, "Titanium Dioxide as the Most Used Photocatalyst for Water Purification: An Overview," *Catalysts*, vol. 13, no. 1, 2023, doi: 10.3390/catal13010026.
8. A. A. Aziz, F. Khatun, M. U. Monir, S. L. Ching, and L. K. Hon, "TiO₂: A Semiconductor Photocatalyst," in *Titanium Dioxide*, H. M. Ali, Ed., Rijeka: IntechOpen, 2021. doi: 10.5772/intechopen.99256.
9. M. Sun, H. Liu, Z. Sun, and W. Li, "Donor-acceptor codoping effects on tuned visible light response of TiO₂," *J. Environ. Chem. Eng.*, vol. 8, no. 5, p. 104168, Oct. 2020, doi: 10.1016/j.jece.2020.104168.
10. W. Zhao, W. Hua, Y. Wang, L. Shi, W.-D. Fei, and Y. Zhao, "Colossal permittivity and ferroelectric properties regulation of different kinds of doped TiO₂," *Ceram. Int.*, vol. 50, no. 12, pp. 21059–21065, June 2024, doi: 10.1016/j.ceramint.2024.03.214.



11. R. D. Shannon, "Revised effective ionic radii and systematic studies of interatomic distances in halides and chalcogenides," *Acta Crystallogr. Sect. A*, vol. 32, no. 5, pp. 751–767, 1976, doi: <https://doi.org/10.1107/S0567739476001551>.
12. F. Wang et al., "Realizing chemical codoping in TiO₂," *Phys Chem Chem Phys*, vol. 17, no. 27, pp. 17989–17994, 2015, doi: [10.1039/C5CP02020D](https://doi.org/10.1039/C5CP02020D).
13. . Wang et al., "Synergistic effect of N-doping and rich oxygen vacancies induced by nitrogen plasma endows TiO₂ superior sodium storage performance," *Electrochimica Acta*, vol. 309, pp. 242–252, June 2019, doi: [10.1016/j.electacta.2019.04.051](https://doi.org/10.1016/j.electacta.2019.04.051).
14. E. N. K. Glover, S. G. Ellington, G. Sankar, and R. G. Palgrave, "The nature and effects of rhodium and antimony dopants on the electronic structure of TiO₂: towards design of Z-scheme photocatalysts," *J Mater Chem A*, vol. 4, no. 18, pp. 6946–6954, 2016, doi: [10.1039/C6TA00293E](https://doi.org/10.1039/C6TA00293E).